Aggregation-Induced Emission Enhancement in Alkoxy-Bridged Binuclear Rhenium(I) Complexes: Application as Sensor for Explosives and Interaction with Microheterogeneous Media

ARTICLE *in* THE JOURNAL OF PHYSICAL CHEMISTRY B · OCTOBER 2013

Impact Factor: 3.3 · DOI: 10.1021/jp407939j · Source: PubMed

7 AUTHORS, INCLUDING:

Sathish Veerasamy
Bannari Amman Institute of Technology
20 PUBLICATIONS **27** CITATIONS
SEE PROFILE

Pounraj Thanasekaran
Academia Sinica
47 PUBLICATIONS **906** CITATIONS
SEE PROFILE

THE JOURNAL OF PHYSICAL CHEMISTRY B

Article

pubs.acs.org/JPCB

Aggregation-Induced Emission Enhancement in Alkoxy-Bridged Binuclear Rhenium(I) Complexes: Application as Sensor for Explosives and Interaction with Microheterogeneous Media

Veerasamy Sathish,[†] Arumugam Ramdass,[†] Zong-Zhan Lu,[‡] Murugesan Velayudham,[‡] Pounraj Thanasekaran,*[,‡] Kuang-Lieh Lu,*[,‡] and Seenivasan Rajagopal*[,†]

[†]School of Chemistry, Madurai Kamaraj University, Madurai 625 021, India

[‡]Institute of Chemistry, Academia Sinica, Taipei 115, Taiwan

Supporting Information

ABSTRACT: The aggregation-induced emission enhancement (AIEE) characteristics of the two alkoxy-bridged binuclear Re(I) complexes $[\{Re(CO)_3(1,4\text{-NVP})\}_2(\mu_2\text{-OR})_2]$ (**1**, R = C_4H_9; **2**, $C_{10}H_{21}$) bearing a long alkyl chain with 4-(1-naphthylvinyl)pyridine (1,4-NVP) ligand are illustrated. These complexes in CH_2Cl_2 (good solvent) are weakly luminescent, but their intensity increased enormously by almost 500 times by the addition of poor solvent (CH_3CN) due to aggregation. By tracking this process via UV−vis absorption and emission spectral and TEM techniques, the enhanced emission is attributed to the formation of nanoaggregates. The nanoaggregate of complex **2** is used as a sensor for nitroaromatic compounds. Furthermore, the study of the photophysical properties of these binuclear Re(I) complexes in cationic, cetyltrimethylammonium bromide (CTAB), anionic, sodium dodecyl sulfate (SDS), and nonionic, *p-tert*-octylphenoxypolyoxyethanol (TritonX-100, TX-100), micelles as well as in CTAB−hexane−water and AOT−isooctane−water reverse micelles using steady-state and time-resolved spectroscopy and TEM analysis reveals that the nanoaggregates became small and compact size.

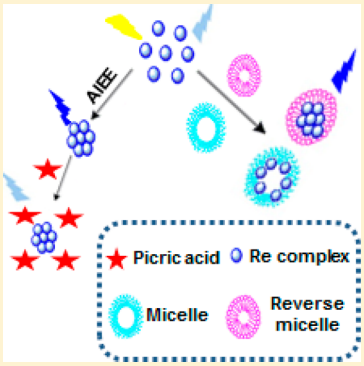

INTRODUCTION

In recent years there has been burgeoning interest in rhenium(I)−tricarbonyl-based metal complexes due to their potential applications as sensors,[1] catalysts,[2] light-emitting devices,[3] optical switches,[4] bioprobes,[5] in CO_2 fixation,[6] and for cellular imaging.[7] They have tremendous rich photophysical and photochemical characteristics such as high stability and fairly strong emission in the visible region.[8] If these metal complexes carry amphiphilic units like long alkyl chains, they can undergo aggregation in aqueous solution to form micelles and vesicles leading to enormous enhancement in luminescence with potential applications.[9,10] We realized this interesting aggregation-induced emission enhancement phenomenon for the first time in the Re(I)−tricarbonyl complexes in the past decade.[11]

The aggregation observed with these amphiphilic molecules with the change of solvent system sometimes may change the luminescent properties enormously, leading to novel applications.[10] This aggregation phenomenon caused by the strong intramolecular $\pi-\pi$ interaction in the solid state may lead to luminescence quenching. This aggregation caused quenching (ACQ) is a spiny problem in the development of OLEDs[12] and in the fluorescence sensing device, particularly sensing of biomolecules,[13] so that there is a huge demand for the development of fluorescent probes without ACQ. To achieve this, it is necessary to develop new luminophoric materials whose aggregates can emit more efficiently than monomers in solution. In this context two unusual phenomena exactly opposite to the ACQ have been identified by Tang et al.:[10,14−17] one is the aggregation-induced emission enhancement (AIEE), and the other is the aggregation-induced emission (AIE). In the former, light emission of a chromophoric material is enhanced by aggregate formation, while in the latter, a nonemissive material is induced to emit by aggregation. Tang et al.[14−17] and others[11] worked on these materials having aggregation-induced emission properties since its inception.

Recently a burst of research activity is witnessed in the area of AIE (E) because of these promising candidates for potential applications in OLED,[16] bioimaging,[17] biosensors for proteins,[18] detection of insulin fibrillation,[19] and recognition of fingerprints.[20] There are numerous reports on the AIE active dyes which include siloles,[21] 1-cyano-*trans*-1,2-bis(4′-methylbiphenyl)ethylene (CN-MBE),[22] 2,5-diphenyl-1,4-distyrylbenzene (DPDSB) derivatives,[23] diphenyldibenzofulvene (DPDBF) derivatives,[24] conjugated polymers,[25] and others.[26] So far AIE(E) has been observed in many organic molecules, but such reports on metal-containing supramolecules are scarce.[27] Our group[28] synthesized a variety of binuclear and tetranuclear complexes containing Re(I) and unearthed the first

Received: August 8, 2013
Revised: October 29, 2013
Published: October 31, 2013

AIEE in metal-containing supramolecules; i.e., alkoxy-bridged Re(I) molecular rectangles displayed AIEE properties and function as a probe for photoluminescence quenching of quinones and amines.[29] On these lines, we have now synthesized two binuclear rhenium(I) complexes comprising long alkyl chains carrying a naphthyl moiety which exhibit excellent photoswitchable, bioprobes, and optical imaging properties[30] in addition to AIEE behavior. In good solvents, these complexes show a very weak luminescence while a strong emission is observed by the addition of poor solvents where these complexes aggregate, resulting in the formation of AIEE.

The study of photophysical and photochemical properties of luminescent probes containing surfactant ligands in micro-heterogeneous media is of great interest because of their extensive applications in mimicking biological systems,[31] in drug delivery,[32] and solar energy conversion and storage.[33] Amphiphilic molecules contain both hydrophobic and hydrophilic parts, and their photophysical properties are highly influenced by the change of solvent and the change in medium from homogeneous to microheterogeneous.[34,35] The optical properties of luminescent probes are strongly affected by the change of polarity and rigidity of their environments.[35] In addition, the structure, dynamics, and reactivity of a probe molecule at the interface differ markedly from those observed in the bulk media due to the change polarity and viscosity.[36] Below the critical micellar concentration (cmc), these probes will exist in aqueous medium, whereas above the cmc they are incorporated into a micelle. Self-association of ionic amphiphiles to micelles is governed by intricate balance between hydrophobic interactions among the nonpolar alkyl chains and the electrostatic interactions of the ionic head groups with themselves, counterions, and water.

Although many reports are available on the use of ruthenium(II) complexes as probes in micellar media,[37−39] such studies on the rhenium(I)−diimine system are very limited.[40,41] Recently Wu et al.[42] reported the hydrogen gas evolution from rhenium(I) complexes in micellar systems using a biomimetic pathway. Herein we report on the novel behavior of binuclear rhenium(I) complexes comprising long alkyl chains (Chart 1) to exhibit AIEE properties, and further we explore their efficacy as fluorescence probes for explosives and for organized assemblies, particularly cationic, anionic, neutral micelles, and CTAB−hexane−water and AOT−isooctane−water reverse micelles.

Chart 1. Structure of Complexes 1 and 2

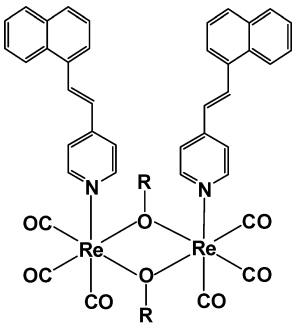

1, R = C_4H_9
2, R = $C_{10}H_{21}$

EXPERIMENTAL SECTION

Materials and Instrumentation. The bimetallic rhenium(I) complexes **1** and **2** were synthesized by one pot self-assembly method from $Re_2(CO)_{10}$ and 4-(1-naphthylvinyl)-pyridine in 1-butanol or 1-decanol and characterized by the spectral and X-ray techniques.[30] Cetyltrimethylammonium bromide (CTAB), sodium dodecyl sulfate (SDS), Triton X-100, and sodium 1,4-bis(2-ethylhexyl)sulfosuccinate (AOT) (99% purity) were procured from Sigma-Aldrich. All nitro aromatic compounds are received from commercial sources and used as received. HPLC grade dichloromethane, acetonitrile, and DMSO were employed in all photophysical and photochemical measurements. Transmission electron microscope (TEM) analysis was performed on a Tecnoi-10-Philips instrument at an 80 kV accelerating voltage.

Caution! The nitroaromatic compounds used in this study, especially picric acid, are very powerful explosives. They must be handled with care and also in very small quantities.

Methods. The stock solution for complexes **1** and **2** (1×10^{-3} M) were prepared in dichloromethane solution for carrying out AIEE studies. For the micellar studies, the complexes **1** and **2** are dissolved in 2% DMSO−98% water (v/v). For reverse micellar studies the microemulsions were prepared by mixing the requisite volume of the stock solution of the complex in water with the calculated amount of double distilled water to yield a required w_0 and calculated quantity (0.5 mL) of 1 M AOT in isooctane solution. The final volume was adjusted with isooctane to yield a final concentration of 0.1 M AOT surfactant in isooctane. The mixture was stirred at room temperature until water was solubilized to form optically transparent uniform solution. The amount of water present in the system was expressed as the molar ratio between water and the surfactant as $w_0 = [H_2O]/[AOT]$. Studies were performed at different w_0 values ranging from 10 to 50.

The concentration of CTAB in all samples is 0.5 M, and spectroscopic grade *n*-hexanol was used as cosurfactant in CTAB/isooctane−*n*-hexanol/water microemulsions. The ratio of isooctane to *n*-hexanol is 9:1, and this ratio is maintained throughout the studies. The cationic reverse micellar solution was prepared in a 10 mL volumetric flask adding 0.183 g of CTAB (0.5 M) to the required volume of aqueous solution as the water pool to maintain the particular w_0 and filling the volumetric flask up to the mark with 9:1 (v/v) mixture of isooctane/*n*-hexanol followed by vortexing for 10−15 s. Studies were performed at seven different w_0 values ranging from 6 to 50. Surfactant to probe concentration is always $>10^3$ to avoid multiple occupancy. Double distilled water was used throughout experiment. The sample solutions were prepared freshly for each measurement.

Photophysical Measurements. The electronic absorption spectrum is recorded on AnalytikJena Specord S100 spectrophotometer using 1 cm path length cuvette. Emission spectra are measured using JASCO FP6300 spectrofluorometer. Excitation and emission slits with a band-pass of 2.5 or 5 nm are used for all measurements. Emission quantum yields are measured in deoxygenated water solution by integration of the corrected emission spectra relative to that of $[Ru(bpy)_3](PF_6)_2$ (Φ = 0.062 in deoxygenated CH_3CN).[43]

Excited State Lifetime Measurement. Fluorescence decays were recorded using the time-correlated single photon counting (TCSPC) method using the following setup. A diode pumped millena CW laser (Spectra-Physics) 532 nm was used

dx.doi.org/10.1021/jp407939j | J. Phys. Chem. B 2013, 117, 14358−14366

to pump Ti:sapphire rod in Tsunami picosecond mode locked laser system (Spectra-Physics). The 750 nm (8 MHz) line was taken from the Ti:sapphire laser and passed through a pulse picker (Spectra-Physics, 3980 2s) to generate 80 kHz pulses. The second harmonic output (375 nm) was generated by a flexible harmonic generator (Spectra-Physics, GWU 23 ps). The vertically polarized 375 nm laser was used to excite the sample. The fluorescence emission at the magic angle (54.7°) was dispersed in a monochromator (f/3 aperture), counted by a MCP PMT (Hamamatsu R 3809), and processed through CFD, time-to-amplitude converter (TAC), and multichannel analyzer (MCA). The instrument response function for this system is ≈52 ps, and the fluorescence decay was analyzed by using the software provided by IBH (DAS-6) and PTI global analysis software.

Transient Absorption Spectral Study. Transient absorption measurements were made with laser flash photolysis technique using an Applied Photophysics SP-Quanta Ray GCR-2(10) Nd:YAG laser as the excitation source (pulse width ~8 ns and energy 50 mJ/pulse). The time dependence of the luminescence decay was observed using a Czerny-Turner monochromator with a stepper motor control and a Hamamatsu R-928 photomultiplier tube. The production of the excited state on exposure to 355 nm was measured by monitoring (pulsed xenon lamp of 250 W) the absorbance change. The change in the absorbance of the sample on laser irradiation was used to calculate the rate constant as well as to record the time-resolved absorption transient spectrum.

RESULTS AND DISCUSSION

The complexes **1** and **2** containing long alkyl chains are insoluble in water and acetonitrile, but they are readily soluble in solvents like dichloromethane and DMSO. The absorption spectra of complexes **1** and **2** recorded in dichloromethane (Figure 1) show an intense band at 235 nm with a shoulder at

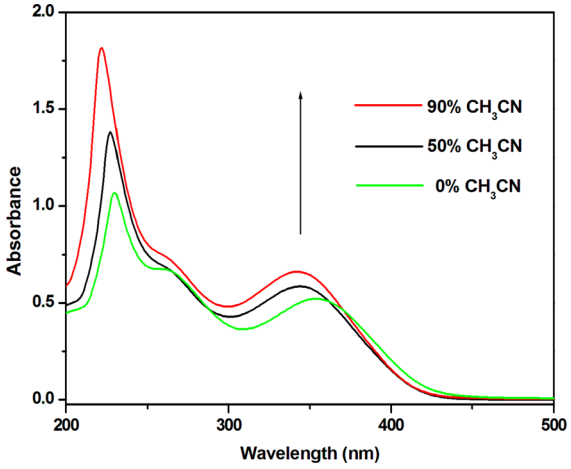

Figure 1. Absorption spectra of complex **2** (20 μM) in CH_2Cl_2 and after the addition of CH_3CN 0, 50, and 90%.

261 nm and a broad band at 355 nm which have been assigned to the ligand-centered (LC) (235 and 261 nm) and metal-to-ligand charge transfer (MLCT) (355 nm) transitions, respectively.

Because of the presence of long alkyl chains and −C≡C− moiety between naphthyl and phenyl groups, we anticipate that when polar solvents (poor solvents), such as acetonitrile, are added, complexes **1** and **2** could form nanoaggregates.[10,11] The formation of aggregates observed in the polar organic solvents rather than water has recently been reported.[44,45] When we added acetonitrile to the complexes **1** and **2** dissolved in dichloromethane, the absorption maximum at 355 nm is blue-shifted by 15 nm with an increase in the absorbance, and the intensity of absorption of ligand centered transition is also increased with a blue-shift by 9 nm from 230 to 221 nm (Figure 1). We propose that the increase in absorption intensity with a blue-shift may be due to the formation of H-aggregates by strong π-stacking interactions of the naphthalene moiety as pointed out in the earlier reports.[22,46,47] Furthermore, the hydrophobic long alkyl chains could induce the formation of nanoaggregates upon increasing the polarity by adding CH_3CN. The solutions are macroscopically homogeneous with no precipitation, even on standing for long periods of time, up to 20 μM concentration of complex **2**. The formation of aggregates by complex **2** has been examined by emission spectral studies. Complex **2** has a weak emission at 420 nm in CH_2Cl_2 when excited at 365 nm. However, upon the incremental addition of acetonitrile to a CH_2Cl_2 solution of complex **2**, an enormous increase in emission intensity by 20-fold is observed without any shift in the λ_{max} value (Figure 2).

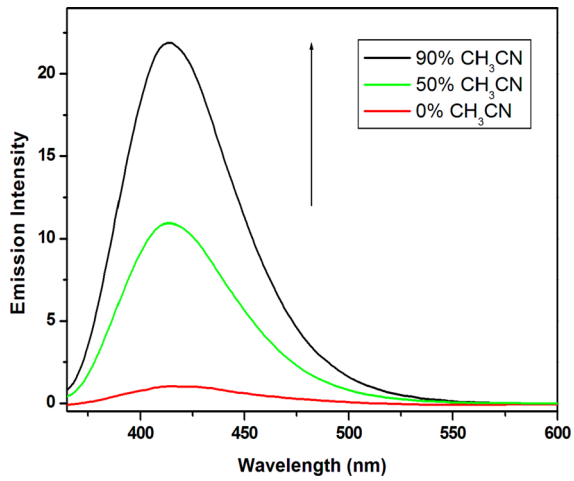

Figure 2. Emission spectra of complex **2** (20 μM) in CH_2Cl_2 (dashed line) and after the addition of CH_3CN 0, 50, and 90%.

The increase in emission intensity may be because of aggregate formation due to π-stacking interactions induced by long alkyl chain that expels the solvent molecules, and the aggregation leads to less vibrational motion, resulting in the suppression of rate of nonradiative decay.[11] Another possibility for this luminescence enhancement is the restriction of intramolecular rotation of the 1,4-NVP ligand in the complex **2** which will prevent the energy loss by the nonradiative decay.[48] Furthermore, the luminescence quantum yield is also increased from 7.4×10^{-4} to 5.2×10^{-3} when CH_3CN (90%) is added. Complex **2** in dichloromethane showed a lifetime of 0.7 ns. Upon the addition of acetonitrile into a dichloromethane solution (CH_2Cl_2:CH_3CN, 10:90 v/v) of **2**, the lifetime value increased to 4.7 ns after 2 h (Figure S1 in the Supporting Information).

To gain further insights into the emission enhancement caused by nanoaggregates, we investigated the time dependence of emission intensity of complex **2** in a CH_2Cl_2−CH_3CN (10:90) mixture. The emission spectrum was recorded after

dx.doi.org/10.1021/jp407939j | J. Phys. Chem. B 2013, 117, 14358−14366

stirring for 5 min. After the addition of acetonitrile into the dichloromethane solution of complex **2** by keeping the concentration of **2** constant, the spectra were recorded at different time intervals up to 2 h, and the details of the change in the emission intensity are shown in Figure 3. From the

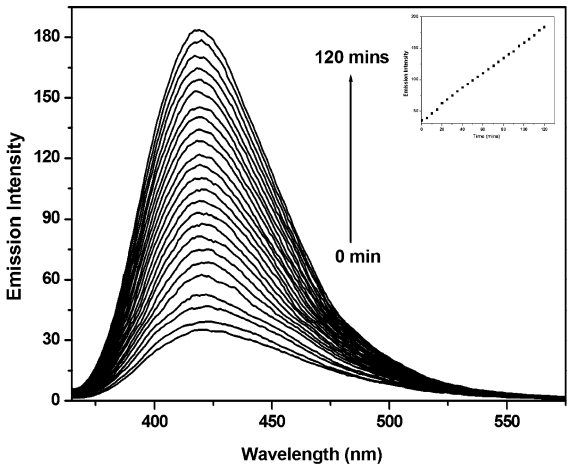

Figure 3. Emission spectra of complex **2** (λ_{ex} = 365 nm) in a CH_2Cl_2–CH_3CN mixture (10:90 v/v) at different aging times. Δt = 5 min, [**2**] = 20 μM (inset: time vs emission intensity spectra of complex **2**).

spectrum shown in Figure 3 we realize that the emission intensity is increased tremendously up to 180-fold after 2 h at room temperature (Figure 3), but the enhancement becomes 500-fold after 1 day (Figure S2 in the Supporting Information), and the rate of fluorescence enhancement is first order with respect to the time. Reports on this kind of fluorescence enhancement with respect to time are available in the literature.[49,50] Qian et al.[51] reported that the time needed for the full growth of nanoparticles during the aggregation process and the strong hydrophobic interactions caused by *tert*-butyl group stimulate the emission enhancement effectively. After aging of time, the fluorescence intensity was no longer intensified but gradually decreased due to the precipitation of larger aggregates in mixed solvents. But in our case, even after 1 day, the emission intensity goes on increasing and the intensity remains stagnant afterward with the solutions macroscopically homogeneous with no precipitation (Figure S2 in Supporting Information). Thus, here also, the enhanced emission is attributed to the aggregation of long alkyl chains to form the clusters of nanoparticles slowly with an increase in time. It is interesting to note that this behavior is observed only for complex **2**, not for complex **1**. It seems that the length of alkyl chain plays a major role in the emission enhancement followed by the formation of nanoaggregates. The formation of nanoscopic aggregates of **2** was confirmed by TEM image studies. Formation of aggregates was not observed in pure CH_2Cl_2 or CH_2Cl_2 with other organic solvents except CH_3CN. However, in the CH_2Cl_2:CH_3CN solvent system, with CH_3CN composition of 90%, complex **2** underwent aggregate formation.

This is because addition of CH_3CN changed significantly the polarity of the medium. These nanoaggregates exhibit normal spherical features with an average size of 100–150 nm (Figure 4). It has been shown that thiol-functionalized poly(amidoamine) containing Re(I) complexes in aqueous solution formed nanoparticles with a spherical morphology ranged from 5 to 12 nm as revealed by TEM analysis.[52] In another study,

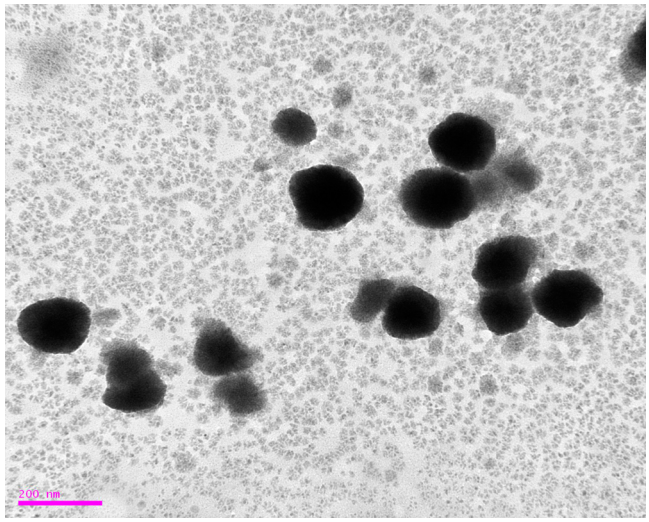

Figure 4. TEM image of nanoaggregates of complex **2** in CH_2Cl_2–CH_3CN mixture (10:90 v/v).

TEM images of acetonitrile-cast films of polymer $\{[(vpy)_2vpyRe(CO)_3(NO_2\text{-phen})^+]\}_{n\sim200}$ (NO_2-phen = 5-nitro-1,10-phenanthroline; vpy = poly(4-vinylpyridine))[53] showed the aggregation of polymer followed by the formation of nanodomains with a dimension of 80–160 nm, whereas it formed branched tubular structures intertwined in a net in dichloromethane-cast film.

Nanoaggregates as Sensor for Explosives. The sensing and removal of trace level explosives is a challenging area, but stupendous efforts are made by the researchers in the field of chemical sensors.[54] Among the various techniques, fluorescence-based sensing offers much simplicity, high sensitivity, specificity, low background noise, wide dynamic ranges, and real time monitoring with short response time.[55]

With this idea in mind, the strong emission of nanoaggregates of complex **2** is used to explore their potential applications in the selective detection of nitroaromatics, such as picric acid (PA), which is used as primary constituent of explosives in unexploded landmines.[56] Picric acid (PA) and other nitroaromatic compounds are employed as model explosives. Recently, some reports are available on the application of nanoaggregates of amphiphilic cellulose,[57] curcumin,[58] and other organic molecules[59,60] to detect the explosives. We used intriguing AIEE behavior of our binuclear rhenium metal complex **2** for sensing nitroaromatics.

We performed the absorbance and luminescence quenching experiments by using the highly emissive nanoaggregates of complex **2** (obtained by keeping **2** in CH_2Cl_2/CH_3CN mixture (10:90 v/v) for 2 h) with various nitroaromatics. Figure S3 in the Supporting Information shows the absorbance spectra of nanoaggregates of **2** with the addition of different amounts of PA. When different [PA] is added to the nanoaggregates of complex **2**, the absorbance is increased and λ_{max} value red-shifted to the tune of 40 nm from 326 to 366 nm. These absorption spectral changes indicate a strong interaction between the host and guest, and it is likely to form a ground state charge transfer complex.

In the luminescence spectra, upon addition of PA into the nanoaggregates of complex **2**, the emission intensity is rapidly quenched without any considerable shift in the emission maximum(Figure 5). At lower concentrations of PA, a plot of I_0/I vs [PA] is linear, and the Stern–Volmer constant (K_{sv}) is

dx.doi.org/10.1021/jp407939j | J. Phys. Chem. B 2013, 117, 14358–14366

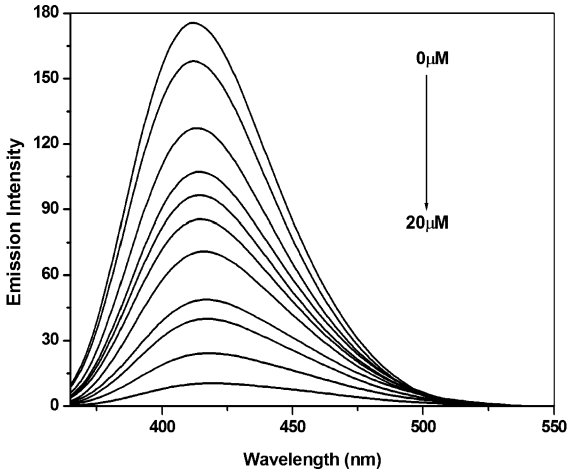

Figure 5. Emission spectra of nanoaggregates of complex **2** (20 μM) in CH_2Cl_2 /CH_3CN mixture (10:90 v/v) containing different amounts of PA.

found to be 1.0 × 10^5 M^{-1} (Figure S4). At higher concentrations of PA, the graph shows an upward curvature, and it may be due to the superamplified quenching effect[61] (Figure S4). These emission spectral changes are attributed to the formation of a charge transfer complex between the electron-poor picric acid (quencher) and electron-rich fluorophore (donor).[62] The quenching experiment of PA with complex **2** after 24 h incubation is also carried out, and the K_{sv} value is 2.3 × 10^5 M^{-1}, which is closely related to the case of nanoaggregates of complex **2** after 2 h (Figure S5). We also examined the quenching efficiency for other nitro derivatives. Interestingly, the selectivity is very high toward picric acid with quenching efficiency of ca. 94% (Figure 6). It confirms that the complex **2** is selectively sensing picric acid compared to the other nitro derivatives.

Effect of Micellar Media. The photophysical and morphological behaviors of complexes **1** and **2** are examined in micellar medium. When the surfactants are added to the aqueous solution (aqueous medium corresponds to 98% H_2O–2% DMSO, (v/v)) of complexes **1** and **2**, a slight change in absorption spectrum is observed. On the addition of CTAB a small increase in the molar extinction coefficient of complex **2** is noticed without any considerable shift in the $^{ab}\lambda_{max}$ value. Similar behavior is observed in the presence of nonionic surfactant, TX-100, and anionic surfactant, SDS. Contrary to this observation in the absorption spectrum, the change in the luminescence intensity of the complexes **1** and **2** upon the addition of surfactant is drastic when the surfactant concentration reached the cmc value which represented the onset of micelle formation.[63] The luminescence intensity of the complexes **1** and **2** showed a significant enhancement on the addition of surfactants (CTAB and TX-100) with the 20 nm blue-shift from 440 nm (in aqueous solution) to 420 nm in the micellar medium (Figure 7 and Figure S12).

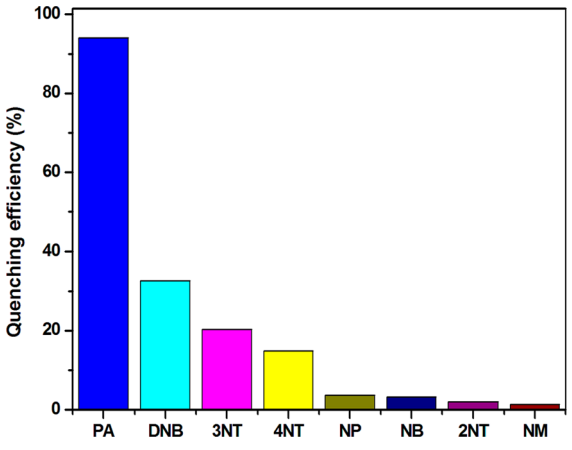

Figure 6. Relative fluorescence quenching of complex **2** upon addition of 20 equiv of various nitro derivatives: PA = picric acid, DNB = 1,4-dinitrobenzene, 3NT = 3-nitrotoluene, 4NT = 4-nitrotoluene, NP = nitrophenol, NB = nitrobenzene, 2NT = 2-nitrotoluene, NM = nitromethane.

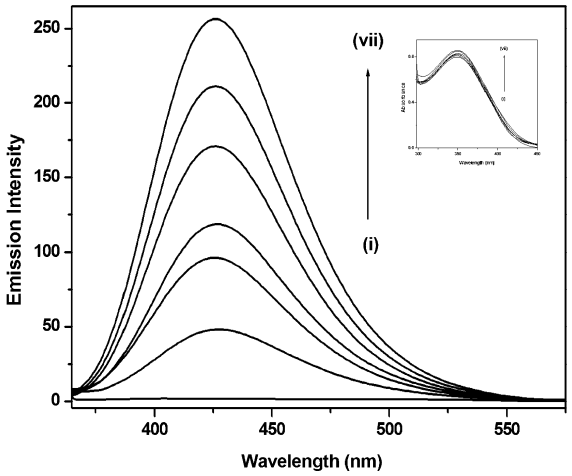

Figure 7. Emission spectra of complex **2** as a function of CTAB concentration (λ_{exc} = 365 nm). Curves i–vii correspond to 0, 0.0002, 0.0005, 0.001, 0.002, 0.005, and 0.01 M CTAB. Inset: absorption spectra of complex **2** with CTAB at above concentrations.

The probe's passage from the polar aqueous medium to less polar site in the micellar environment reduces nonradiative decay rate and hence changes the emission maximum along with intensity. These spectral changes confirm the strong binding of complexes **1** and **2** with surfactants due to hydrophobic interactions between the micelles and the long alkyl chains in **1** and **2**.[64] Interestingly, the emission intensity of complex **2** with SDS micelles is red-shifted by 65 nm from 440 to 505 nm (Figure S13). We propose that this red-shifted luminescence in SDS micelles is due to the formation of J-like nanoaggregates. Such substantial red-shift in the luminescence maximum due to J-aggregates has been reported previously.[65]

The enhancement of fluorescence intensity of complexes **1** and **2** in micellar solution can be rationalized in terms of the binding of the probe with the micelle. Almgren et al.[66] have used eq 1 for the estimation of binding constant (K) between the probe and micelle from the fluorescence intensity data:

$$(I_\infty - I_0)/(I_t - I_0) = 1 + (K[M])^{-1} \quad (1)$$

where I_∞, I_0, and I_t are the relative intensities under complete micellization, in the absence of surfactant, and in the presence of intermediate amounts of surfactants, respectively. [M] represents the concentration of micelle which is given by the equation

$$[M] = ([Surf] - cmc)/N \quad (2)$$

dx.doi.org/10.1021/jp407939j | J. Phys. Chem. B 2013, 117, 14358–14366

[Surf] represents the surfactant concentration, and N is the aggregation number of the micelle. The N values used in the calculation of [M] are 62, 60, and 143 for SDS, CTAB, and Triton X-100, respectively.

The binding constant values of complex **2** with micelles are calculated from eq 1, and the values are found to be 3.2×10^4, 2.9×10^4, and 5.4×10^4 M^{-1} for CTAB, SDS, and TX-100, respectively (Table 1). These results show that the binding is strongest with the nonionic micelle which may be due to more stabilization of the probe in nonionic as well as nonpolar (hydrophobic) environment compared to ionic micelles. Fluorescence lifetime serves as a sensitive indicator of the local environment in which a given fluorophore is placed, and it has the information about the unique insights into the systems.[67] Figure S14 shows the luminescence decay of complex **2** in the absence and in the presence of CTAB and TX-100 micelles. The fluorescence lifetime of the complexes also increases with the increasing concentration of the surfactants. In aqueous medium the complex has biexponential decay with lifetime of less than 1 ns. After the addition of the surfactants it slightly increases with the biexponential decay with lifetime 2.2 and 2.7 ns in the presence of CTAB and TX-100, respectively. The transient spectrum of complex **2** in the presence of TX-100 micelle shows absorption around 380 nm which corresponds to MLCT transition, and the 550 nm absorption maximum is assigned to the intramolecular triplet monomer of the naphthalene moiety[68] (Figure S15).

Table 1. Binding Constant for Re(I) Binuclear Complexes 1 and 2 with Different Micelles at 298 K

compd	CTAB ($\times 10^4$ M^{-1})	SDS ($\times 10^4$ M^{-1})	TX-100 ($\times 10^4$ M^{-1})
1	3.4	3.3	5.1
2	3.2	2.9	5.4

Figure 8 shows the TEM image of complex **2** in the presence of 0.005 M CTAB. This TEM study reveals that the complex **2** with CTAB micelles forms the nanoparticles of spherical shape with average diameter size of 30−50 nm.

Effect of Reverse Micelles. Reverse micelles (RM) are the aggregates of the surfactants formed in a nonpolar solvent. They are thermodynamically stable and isotropic systems that are constituted by water, oil, and one or more surfactants.[69] Reverse micelles find applications as nanoreactors, as medium for excited state proton transfer, as templates for nanoparticles, and as model for biological membranes because of their ability to serve as hydrophilic components in organic solvents.[70] Recently Axelsen et al.[71] reported that the reverse micelles mimic the Aβ40 monomers and induce the formation of amyloid fibrils. In complex **2** there is a considerable shift in the peak position of the emission spectrum and an enormous increase in the emission intensity of the complex when the medium is changed from bulk water to AOT/isooctane reverse micelle.

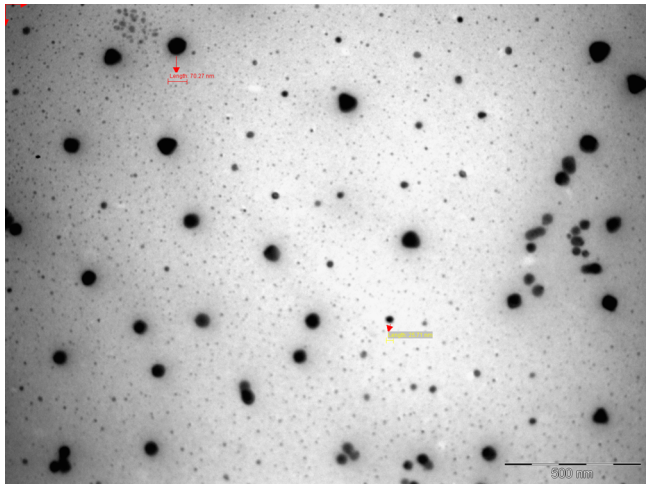

Figure 8. TEM image of aggregate of complex **2** in the presence of CTAB micelle.

Figure 9 shows that the emission spectrum of complex **2** has two maxima: one in AOT/isooctane/water reverse micelles at 390 nm and the other in homogeneous aqueous medium at 410 nm. Upon increasing water loading, the emission intensity of complex **2** is decreased which is attributed to the increase in the micropolarity of the RM surface. When the complex **2** is in aqueous medium, the emission spectrum shows a single band at 440 nm, but dual emission at 390 and 410 nm is observed in the AOT RM medium. On the other hand, in the cationic CTAB/isooctane/hexanol reverse micellar medium the complex **2** shows a single emission at 397 nm rather than dual fluorescence (Figure S16). The structure of complex **2** in the presence of AOT reverse micelle is pictorially represented in Figure S17. Since the headgroup of AOT reverse micelle carries negative charge, it is proposed that the Re(I) part of complex **2** is at the interface and long alkyl chain and aromatic part are projected toward the hydrophobic region.

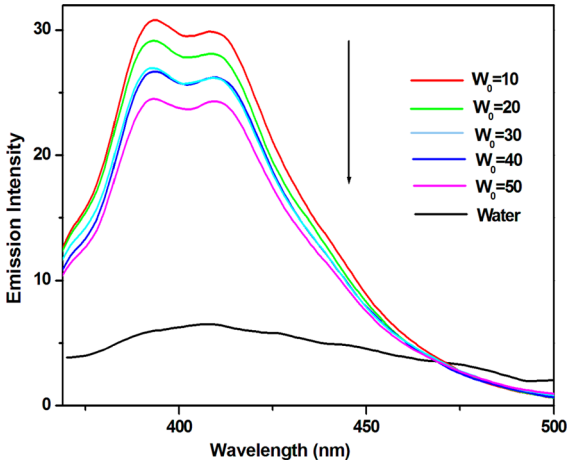

Figure 9. Emission spectra of **2** in water and AOT/isooctane/water reverse micelle at various w_0.

Thus, the dual emission observed in the presence of AOT may be due to the presence of two different regions one at the interface and the another at the hydrophobic region. In the case of CTAB reverse micelle the probe is expected to reside only at the hydrophobic region and not at the interface due to electrostatic repulsion. The formation of micellar aggregates is confirmed by TEM images. The sample micellar/reverse micellar solution was placed on a carbon support film on a copper grid, and the grids were dried in a vacuum for 5 min. The TEM image of complex **2** in the presence of 0.005 M CTAB shows that the complex **2** with CTAB micelles forms the nanoparticles of spherical shape with average diameter size of 30−50 nm. But in the CTAB/hexane/water reverse micelles

dx.doi.org/10.1021/jp407939j | J. Phys. Chem. B 2013, 117, 14358−14366

(w_0 = 20) we see that the aggregates are in the distorted spherical shape, and they are arranged very closely together with the average diameter size of 30−70 nm (Figure 10). These

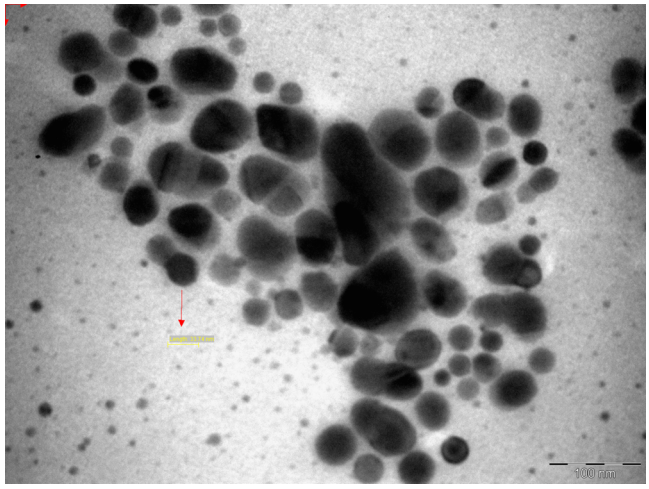

Figure 10. TEM image of the aggregate of complex **2** in CTAB/hexane/water reverse micelle at w_0 = 20.

results are in reasonable agreement[72,73] with the previous observations that the formation, nature, and size of the nanostructures of the complex **2** vary with the micelles and reverse micelles. From these observations, we propose that the nanoparticles are small and compact size in the presence of surfactants.[74]

CONCLUSION

Our current results demonstrate that the binuclear rhenium(I) complexes comprising long alkyl chains with photoswitchable 4-(1-naphthylvinyl)pyridine ligand exhibit AIEE characteristics and serve as excellent probe for micelles and reverse micelles. Since the discovery of AIEE phenomena, only seldom reports are appeared on the AIE properties of rhenium(I)−tricarbonyl-based metal complexes and interactions with micellar media. So we take on this perspective and successfully exhibited AIEE properties, and they are highly sensitive to the change of medium from aqueous to microheterogeneous. It is suggested that when these molecules are placed in poor solvents, the enhancement of emission is induced by aggregation with changing the time and in aqueous medium it strongly binds with micelles as well as reverse micelles due to hydrophobic interactions. Furthermore, we anticipate to explore further research on these binuclear systems as probes for sensing and/or inhibiting the aggregation of proteins which is responsible for neurodegenerative disorders such as Alzheimer, Parkinson, Huntington's diseases, and type 2 diabetes.

ASSOCIATED CONTENT

Supporting Information

Lifetime decay of complex **2** in different solvent mixture, absorption spectra and Stern−Volmer plot of complex **2** with picric acid, UV−vis and emission spectra of complex **1** with different micelles; full names of refs 19, 21, 23, and 24. This material is available free of charge via the Internet at http://pubs.acs.org.

AUTHOR INFORMATION

Corresponding Authors

*E-mail rajagopalseenivasan@yahoo.com (S.R.).
*E-mail kllu@gate.sinica.edu.tw (K.-L.L.).
*E-mail ptsekaran@yahoo.com (P.T.).

Notes

The authors declare no competing financial interest.

ACKNOWLEDGMENTS

We thank the Department of Science and Technology (DST)-National Science Council (NSC) for Joint research project funding under Indo-Taiwan S&T Programme. Prof. Lu acknowledges the financial support from Academia Sinica and the NSC of Taiwan. V.S is the recipient of UGC Meritorious fellowship under the Basic Scientific Research (BSR) Scheme. The authors thank Prof. P. Ramamurthy, Director, NCUFP, University of Madras, Chennai, for his help in the TCSPC and laser flash photolysis. For TEM measurements, Dr. G. Gnanakumar is gratefully acknowledged.

REFERENCES

(1) Kumar, A.; Sun, S. S.; Lees, A. J. Directed Assembly Metallocyclic Supramolecular Systems for Molecular Recognition and Chemical Sensing. *Coord. Chem. Rev.* **2008**, *252*, 922−939.

(2) Kuninobu, Y.; Takai, K. Organic Reactions Catalyzed by Rhenium Carbonyl Complexes. *Chem. Rev.* **2011**, *111*, 1938−1953.

(3) Mauro, M.; Yang, C. H.; Shin, C. Y.; Panigati, M.; Chang, C. H.; D'Alfonso, G.; De Cola, L. Phosphorescent Organic Light-Emitting Diodes with Outstanding External Quantum Efficiency Using Dinuclear Rhenium Complexes as Dopants. *Adv. Mater.* **2012**, *24*, 2054−2058.

(4) Lin, J. L.; Chen, C. W.; Sun, S. S.; Lees, A. J. Photoswitching Tetranuclear Rhenium(I) Tricarbonyl Diimine Complexes with a Stilbene-like Bridging Ligand. *Chem. Commun.* **2011**, *47*, 6030−6032.

(5) Lo, K. K.-W.; Choi, A. W.-T.; Law, W. H.-T. Applications as Luminescent Inorganic and Organometallic Transition Metal Complexes as Biomolecular and Cellular probes. *Dalton Trans.* **2012**, *41*, 6021−6047.

(6) Benson, E. E.; Kubiak, C. P. Structural Investigations into the Deactivation Pathway of the CO_2 Reduction Electrocatalyst Re(bpy)-$(CO)_3$Cl. *Chem. Commun.* **2012**, *48*, 7374−7376.

(7) Balasingham, R. G.; Greenwood, F. L. T.; Williams, C. F.; Coogan, M. P.; Pope, S. J. A. Biologically Compatible, Phosphorescent Dimetallic Rhenium Complexes Linked through Functionalized Alkyl Chains: Syntheses, Spectroscopic Properties, and Applications in Imaging Microscopy. *Inorg. Chem.* **2012**, *51*, 1419−1426.

(8) Balzani, V., Scandola, F., Eds.; *Supramolecular Photochemistry*; Ellis Horwood: Chichester, UK, 1991.

(9) Wang, C.; Wang, Z.; Zhang, X. Amphiphilic Building Blocks for Self-Assembly: From Amphiphiles to Supra-amphiphiles. *Acc. Chem. Res.* **2012**, *45*, 608−618.

(10) Luo, J.; Xie, Z.; Lam, J. W. Y.; Cheng, L.; Chen, H.; Qiu, C.; Kwok, H. S.; Zhan, X.; Liu, Y.; Zhu, D.; Tang, B. Z. Aggregation-Induced Emission of 1-Methyl-1,2,3,4,5-pentaphenylsilole. *Chem. Commun.* **2001**, 1740−1741.

(11) Manimaran, B.; Thanasekaran, P.; Rajendran, T.; Lin, R. J.; Chang, I. J.; Lee, G. H.; Peng, S. M.; Rajagopal, S.; Lu, K. L. Luminescence Enhancement Induced by Aggregation of Alkoxy-Bridged Rhenium(I) Molecular Rectangles. *Inorg. Chem.* **2002**, *41*, 5323−5325.

(12) Tang, C. W.; Vanslyke, S. A. Organic Electroluminescent Diodes. *Appl. Phys. Lett.* **1987**, *51*, 913−915.

(13) Suzuki, Y.; Yokoyama, K. Design and Synthesis of Intramolecular Charge Transfer-Based Fluorescent Reagents for the Highly-Sensitive Detection of Proteins. *J. Am. Chem. Soc.* **2005**, *127*, 17799−17802.

(14) Zeng, Q.; Li, Z.; Dong, Y.; Di, C.; Qin, A.; Hong, Y.; Ji, L.; Zhu, Z.; Jim, C. K. W.; Yu, G.; Li, Q.; Li, Z.; Liu, Y.; Qin, J.; Tang, B. Z. Fluorescence Enhancements of Benzene-Cored Luminophors by Restricted Intramolecular Rotations: AIE and AIEE Effects. *Chem. Commun.* **2007**, 70−72.
(15) Hong, Y.; Lam, J. W. Y.; Tang, B. Z. Aggregation-Induced Emission. *Chem. Soc. Rev.* **2011**, *40*, 5361−5368.
(16) Zhao, Z.; Chen, S.; Chan, C. Y. K.; Lam, J. W. Y.; Jim, C. K. W.; Lu, P.; Chang, Z.; Kwok, H. S.; Qiu, H.; Tang, B. Z. A Facile and Versatile Approach to Efficient Luminescent Materials for Applications in Organic Light-Emitting Diodes. *Chem.−Asian J.* **2012**, *7*, 484−488.
(17) Leung, C. W. T.; Hong, Y.; Chen, S.; Zhao, E.; Lam, J. W. Y.; Tang, B. Z. A Photostable AIE Luminogen for Specific Mitochondrial Imaging and Tracking. *J. Am. Chem. Soc.* **2013**, *135*, 62−65.
(18) Ding, D.; Li, K.; Liu, B.; Tang, B. Z. Bioprobes Based AIE Fluorogens. *Acc. Chem. Res.* DOI: 10.1021/ar3003464.
(19) Hong, Y.; Meng, L.; Chen, S.; Leung, C. W. T.; Da, L. T.; Faisal, M.; Silva, D. A.; Liu, J.; Lam, J. W. Y.; Huang, X.; et al. Monitoring and Inhibition of Insulin Fibrillation by a Small Organic Fluorogen with Aggregation-Induced Emission Characteristics. *J. Am. Chem. Soc.* **2012**, *134*, 1680−1684.
(20) Li, Y.; Xu, L.; Su, B. Aggregation Induced Emission for the Recognition of Latent Fingerprints. *Chem. Commun.* **2012**, *48*, 4109−4111.
(21) Li, Z.; Dong, Y. Q.; Lam, J. W. Y.; Sun, J.; Qin, A.; Haußler, M.; Dong, Y. P.; Sung, H. H. Y.; Williams, I. D.; Kwok, H. S.; et al. Functionalized Siloles: Versatile Synthesis, Aggregation-Induced Emission, and Sensory and Device Applications. *Adv. Funct. Mater.* **2009**, *19*, 905−917.
(22) An, B.-K.; Kwon, S.-K.; Jung, S.-D.; Park, S. Y. Enhanced Emission and Its Switching in Fluorescent Organic Nanoparticles. *J. Am. Chem. Soc.* **2002**, *124*, 14410−14415.
(23) Xie, Z.; Yang, B.; Xie, W.; Liu, L.; Shen, F.; Wang, H.; Yang, X.; Wang, Z.; Li, Y.; Hanif, M.; et al. A Class of Nonplanar Conjugated Compounds with Aggregation-Induced Emission: Structural and Optical Properties of 2,5-Diphenyl-1,4-distyrylbenzene Derivatives with All Cis Double Bonds. *J. Phys. Chem. B* **2006**, *110*, 20993−21000.
(24) Tong, H.; Dong, Y.; Hong, Y.; Haussler, M.; Lam, J. W. Y.; Sung, H. H.-Y.; Yu, X.; Sun, J.; Williams, I. D.; Kwok, H. S.; et al. Aggregation-Induced Emission: Effects of Molecular Structure, Solid-State Conformation, and Morphological Packing Arrangement on Light-Emitting Behaviors of Diphenyldibenzofulvene Derivatives. *J. Phys. Chem. C* **2007**, *111*, 2287−2294.
(25) Deans, R.; Kim, J.; Machacek, M. R.; Swager, T. M. A Poly(p-phenyleneethynylene) with a Highly Emissive Aggregated Phase. *J. Am. Chem. Soc.* **2000**, *122*, 8565−8566.
(26) Shustova, N. B.; McCarthy, B. D.; Dincă, M. Turn-On Fluorescence in Tetraphenylethylene-Based Metal−Organic Frameworks: An Alternative to Aggregation-Induced Emission. *J. Am. Chem. Soc.* **2011**, *133*, 20126−20129.
(27) Procopio, E. Q.; Mauro, M.; Panigati, M.; Donghi, D.; Mercandelli, P.; Sironi, A.; D'Alfonso, G.; Decola, L. Highly Emitting Concomitant Polymorphic Crystals of a Dinuclear Rhenium Complex. *J. Am. Chem. Soc.* **2010**, *132*, 14397−14399.
(28) Thanasekaran, P.; Lee, C. C.; Lu, K. L. One-Step Orthogonal-Bonding Approach to the Self-Assembly of Neutral Rhenium-Based Metallacycles: Synthesis, Structures, Photophysics, and Sensing Applications. *Acc. Chem. Res.* **2012**, *45*, 1403.
(29) Thanasekaran, P.; Wu, J. Y.; Manimaran, B.; Rajendran, T.; Chang, I. J.; Rajagopal, S.; Lee, G. H.; Peng, S. M.; Lu, K. L. Aggregate of Alkoxy-Bridged Re(I)-Rectangles as a Probe for Photoluminescence Quenching. *J. Phys. Chem. A* **2007**, *111*, 10953−10960.
(30) Sathish, V.; Babu, E.; Ramdass, A.; Lu, Z.-Z.; Chang, T. T.; Velayudham, M.; Thanasekaran, P.; Lu, K. L.; Li, W. S.; Rajagopal, S. Photoswitchable Alkoxy-Bridged Binuclear Rhenium(I) Complexes − A Potential Probe for Biomolecules and Optical Cell Imaging. *RSC Adv.* **2013**, *3*, 18557−18566.
(31) Gupta, C.; Daechsel, A. K.; Chauhan, A. Interaction of Ionic Surfactants with Cornea-Mimicking Anionic Liposomes. Interaction of Ionic Surfactants with Cornea-Mimicking Anionic Liposomes. *Langmuir* **2011**, *27*, 10840−10847.
(32) Kim, W.; Xiao, J.; Chaikof, E. L. Recombinant Amphiphilic Protein Micelles for Drug Delivery. *Langmuir* **2011**, *27*, 14329−14334.
(33) Yin, J.-F.; Velayudham, M.; Bhattacharya, D.; Lin, H.-C.; Lu, K.-L. Structure Optimization of Ruthenium Photosensitizers for Efficient Dye-Sensitized Solar Cells − A Goal Toward a "Bright" Future. *Coord. Chem. Rev.* **2012**, *256*, 3008−3035.
(34) Mandal, S.; Rao, V. G.; Ghatak, C.; Pramanik, R.; Sarkar, S.; Sarkar, N. Photophysics and Photodynamics of 1′-Hydroxy-2′-acetonaphthone (HAN) in Micelles and Nonionic Surfactants Forming Vesicles: a Comparative Study of Different Microenvironments of Surfactant Assemblies. *J. Phys. Chem. B* **2011**, *115*, 12108−12119.
(35) Mahata, A.; Sarkar, D.; Bose, D.; Ghosh, D.; Girigoswami, A.; Das, P.; Chattopadhyay, N. Photophysics and Rotational Dynamics of a Carboline Analogue in Nonionic Micelles: Effect of Variation of Length of the Headgroup and the Tail of the Surfactant. *J. Phys. Chem. B* **2009**, *113*, 7517−7526.
(36) Li, M.; Chen, Z.; Yam, V. W. W.; Zu, Y. Multifunctional Ruthenium(II) Polypyridine Complex-Based Core−Shell Magnetic Silica Nanocomposites: Magnetism, Luminescence, and Electrochemiluminescence. *ACS Nano* **2008**, *2*, 905−912.
(37) Martinez, A. G.; Vida, Y.; Gutierrez, D. D.; Albuquerque, R. Q.; De Cola, L. Tuning Emission Properties of Iridium and Ruthenium Metallosurfactants in Micellar Systems. *Inorg. Chem.* **2008**, *47*, 9131−9133.
(38) Dressick, W. J.; Cline, J.; Demas, J. N.; DeGraff, B. A. Energy Degradation Pathways and Binding Site Environment of Micelle Bound Ruthenium(II) Photosensitizers. *J. Am. Chem. Soc.* **1986**, *108*, 7567−7574.
(39) Hauenstein, B. L.; Dressick, W. J.; Gilbert, T. B.; Demas, J. N.; DeGraff, B. A. Interactions of Ruthenium(II) Photosensitizers with Non-Ionic Surfactants: The Binding Region and Specific-Anion Effects. *J. Phys. Chem.* **1984**, *88*, 1902−1905.
(40) Blanco, N. G.; Osoro, M. J.; Siles, M. C.; Maldonado, C. R.; Lacey, M. H.; Padro, D.; Clark, S.; Rivas, J. C. M. Iron Oxide-Filled Micelles as Ligands for *fac*-$[M(CO)_3]^+$(M = ^{99m}Tc, Re). *Chem. Commun.* **2012**, *48*, 4211−4213.
(41) Yam, V. W. W.; Lau, V. C. Y.; Wang, K. Z.; Cheunga, K. K.; Huang, C. H. Synthesis, Photophysics, Photochemistry, Electrochemistry and Structural Studies of Luminescent Rhenium(I) Surfactant Complexes; Non-linear Optical Properties in Langmuir−Blodgett Films. *J. Mater. Chem.* **1998**, *8*, 89−97.
(42) Wang, H. Y.; Wang, W. G.; Si, G.; Wang, F.; Tung, C. H.; Wu, L. Z. Photocatalytic Hydrogen Evolution from Rhenium(I) Complexes to [FeFe] Hydrogenase Mimics in Aqueous SDS Micellar Systems: A Biomimetic Pathway. *Langmuir* **2010**, *26*, 9766−9771.
(43) Crosby, G. A.; Demas, J. N. Measurement of Photoluminescence Quantum Yields. Review. *J. Phys. Chem.* **1971**, *75*, 991.
(44) Chien, R. H.; Lai, C. T.; Hong, J. L. Hydrogen Bonds and Enhanced Aggregation Emission of Organic and Polymeric Fluorophores with Alternative Fluorene and Naphthol Units. *J. Phys. Chem. C* **2011**, *115*, 12358−12366.
(45) Yuan, C. X.; Tao, X. T.; Wang, L.; Yang, J. X.; Jiang, M. H. Fluorescent Turn-On Detection and Assay of Protein Based on Lambda (Λ)-Shaped Pyridinium Salts with Aggregation-Induced Emission Characteristics. *J. Phys. Chem. C* **2009**, *113*, 6809−6814.
(46) Karukstis, K. K.; Perelman, L. A.; Wong, W. K. Spectroscopic Characterization of Azo Dye Aggregation on Dendrimer Surfaces. *Langmuir* **2002**, *18*, 10363−10371.
(47) Whitten, D. G.; Chen, L.; Geiger, H. C.; Perlstein, J.; Song, X. Self-Assembly of Aromatic-Functionalized Amphiphiles: The Role and Consequences of Aromatic−Aromatic Noncovalent Interactions in Building Supramolecular Aggregates and Novel Assemblies. *J. Phys. Chem. B* **1998**, *102*, 10098−10111.
(48) Wang, F.; Wen, J.; Huang, L.; Huang, J.; Ouyang, J. A Highly Sensitive "Switch-On" Fluorescent Probe for Protein Quantification

and Visualization Based on Aggregation-Induced Emission. *Chem. Commun.* **2012**, *48*, 7395−7397.
(49) Feng, X.; Tong, B.; Shen, J.; Shi, J.; Han, T.; Chen, L.; Zhi, J.; Lu, P.; Ma, Y.; Dong, Y. Aggregation-Induced Emission Enhancement of Aryl-Substituted Pyrrole Derivatives. *J. Phys. Chem. B* **2010**, *114*, 16731−16736.
(50) Han, Q.; Su, Q.; Tang, L.; Feng, J.; Lu, P.; Wang, Y. Electron Transfer and Aggregate Formation Coinduced Emission Enhancement of 9-Cycloheptatrienylidene Fluorenes in the Presence of Cupric Chloride. *J. Phys. Chem. C* **2010**, *114*, 18702−18711.
(51) Qian, Y.; Li, S.; Zhang, G.; Wang, Q.; Wang, S.; Xu, H.; Li, C.; Li, Y.; Yang, G. Aggregation-Induced Emission Enhancement of 2-(2′-Hydroxyphenyl)benzothiazole-Based Excited-State Intramolecular Proton-Transfer Compounds. *J. Phys. Chem. B* **2007**, *111*, 5861−5868.
(52) Donghi, D.; Maggioni, D.; D'Alfonso, G.; Amigoni, F.; Ranucci, E.; Ferruti, P.; Manfredi, A.; Fenili, F.; Bisazza, A.; Cavalli, R. Tricarbonyl−Rhenium Complexes of a Thiol-Functionalized Amphoteric Poly(amidoamine). *Biomacromolecules* **2009**, *10*, 3273−3282.
(53) Bracco, L. L. B.; Juliarena, M. P.; Ruiz, G. T.; Feliz, M. R.; Ferraudi, G. J.; Wolcan, E. Resonance Energy Transfer in the Solution Phase Photophysics of−$Re(CO)_3L^+$ Pendants Bonded to Poly(4-vinylpyridine). *J. Phys. Chem. B* **2008**, *112*, 11506−11516.
(54) Salinas, Y.; Manez, R. M.; Marcos, M. D.; Sancenon, F.; Costero, A. M.; Parra, M.; Gil, S. Optical Chemosensors and Reagents to Detect Explosives. *Chem. Soc. Rev.* **2012**, *41*, 1261−1296.
(55) Lai, C.-Y.; Trewyn, B. G.; Jeftinija, D. M.; Jeftinija, K.; Xu, S.; Jeftinija, S.; Lin, V. S.-Y. A Mesoporous Silica Nanosphere-Based Carrier System with Chemically Removable CdS Nanoparticle Caps for Stimuli-Responsive Controlled Release of Neurotransmitters and Drug Molecules. *J. Am. Chem. Soc.* **2003**, *125*, 4451−4459.
(56) Toal, S. J.; Trogler, W. C. Polymer Sensors for Nitroaromatic Explosives Detection. *J. Mater. Chem.* **2006**, *16*, 2871−2883.
(57) Wang, X.; Guo, Y.; Li, D.; Chen, H.; Sun, R.-C. Fluorescent Amphiphilic Cellulose Nanoaggregates for Sensing Trace Explosives in Aqueous Solution. *Chem. Commun.* **2012**, *48*, 5569−5571.
(58) Pandya, A.; Goswami, H.; Lodhaband, A.; Menon, S. K. A Novel Nanoaggregation Detection Technique of TNT Using Selective and Ultrasensitive Nanocurcumin as a Probe. *Analyst* **2012**, *137*, 1771−1774.
(59) Bhalla, V.; Gupta, A.; Kumar, M. Fluorescent Nanoaggregates of Pentacenequinone Derivative for Selective Sensing of Picric Acid in Aqueous Media. *Org. Lett.* **2012**, *14*, 3112−3115.
(60) Li, D.; Liu, J.; Kwok, R. T. K.; Liang, Z.; Tang, B. Z.; Yu, J. Supersensitive Detection of Explosives by Recyclable AIE Luminogen-Functionalized Mesoporous Materials. *Chem. Commun.* **2012**, *48*, 7167−7169.
(61) Wang, J.; Mei, J.; Yuan, W.; Lu, P.; Qin, A.; Sun, J.; Ma, Y.; Tang, B. Z. Hyperbranched Polytriazoles with High Molecular Compressibility: Aggregation-Induced Emission and Superamplified Explosive Detection. *J. Mater. Chem.* **2011**, *21*, 4056−4059.
(62) Shanmugaraju, S.; Joshi, S. A.; Mukherjee, P. S. Self-Assembly of Metallamacrocycles Using a Dinuclear Organometallic Acceptor: Synthesis, Characterization, and Sensing Study. *Inorg. Chem.* **2011**, *50*, 11736−11745.
(63) Saroja, G.; Ramachandram, B.; Saha, S.; Samanta, A. The Fluorescence Response of a Structurally Modified 4-Aminophthalimide Derivative Covalently Attached to a Fatty Acid in Homogeneous and Micellar Environments. *J. Phys. Chem. B* **1999**, *103*, 2906−2911.
(64) Rajendran, T.; Rajagopal, S.; Srinivasan, C.; Ramamurthy, P. Micellar Effect on the Photoinduced Electron-Transfer Reactions of Ruthenium(II)−Polypyridyl Complexes with Phenolate Ions. Effect of Cetyltrimethylammoniumchloride. *J. Chem. Soc., Faraday Trans.* **1997**, *93*, 3155−3160.
(65) Rainò, G.; Stöferle, T.; Park, C.; Kim, H.-C.; Chin, I.-J.; Miller, R. D.; Mahrt, R. F. Dye Molecules Encapsulated in a Micelle Structure: Nano-Aggregates with Enhanced Optical Properties. *Adv. Mater.* **2010**, *22*, 3681−3684.
(66) Almgren, M.; Grieser, F.; Thomas, J. K. Dynamic and Static Aspects of Solubilization of Neutral Arenes in Ionic Micellar Solutions. *J. Am. Chem. Soc.* **1979**, *101*, 279−291.
(67) Kumbhakar, M.; Singh, P. K.; Nath, S.; Bhasikuttan, A. C.; Pal, H. Ultrafast Bimolecular Electron Transfer Dynamics in Micellar Media. *J. Phys. Chem. B* **2008**, *112*, 6646−6652.
(68) Wang, X.; Kofron, W. G.; Kong, S.; Rajesh, C. S.; Modarelli, D. A.; Lim, E. C. Transient Absorption Probe of Intermolecular Triplet Excimer of Naphthalene in Fluid Solutions: Identification of the Species Based on Comparison to the Intramolecular Triplet Excimers of Covalently-Linked Dimers. *J. Phys. Chem. A* **2000**, *104*, 1461−1465.
(69) Correa, N. M.; Silber, J. J.; Riter, R. E.; Levinger, N. E. Nonaqueous Polar Solvents in Reverse Micelle Systems. *Chem. Rev.* **2012**, *112*, 4569−4602.
(70) Setua, P.; Ghatak, C.; Rao, V. G.; Das, S. K.; Sarkar, N. Dynamics of Solvation and Rotational Relaxation of Coumarin 480 in Pure Aqueous-AOT Reverse Micelle and Reverse Micelle Containing Different-Sized Silver Nanoparticles Inside Its Core: A Comparative Study. *J. Phys. Chem. B* **2012**, *116*, 3704−3712.
(71) Yeung, P. S.-W.; Axelsen, P. H. The Crowded Environment of a Reverse Micelle Induces the Formation of β-Strand Seed Structures for Nucleating Amyloid Fibril Formation. *J. Am. Chem. Soc.* **2012**, *134*, 6061−6063.
(72) Wolcan, E.; Alessandrini, J. L.; Feliz, M. R. On the Quenching of $MLCT_{Re\rightarrow bpy}$ Luminescence by Cu(II) Species in Re(I) Polymer Micelles. *J. Phys. Chem. B* **2005**, *109*, 22890−22898.
(73) Hou, S.; Man, K. Y. K.; Chan, W. K. Nanosized Micelles Formed by the Self-assembly of Amphiphilic Block Copolymers with Luminescent Rhenium Complexes. *Langmuir* **2003**, *19*, 2485−2490.
(74) Lai, C.-T.; Chien, R.-H.; Kuo, S.-W.; Hong, J.-L. Tetraphenylthiophene-Functionalized Poly(N-isopropylacrylamide): Probing LCST with Aggregation-Induced Emission. *Macromolecules* **2011**, *44*, 6546−6556.